This Accepted Manuscript has not been copyedited and formatted. The final version may differ from this version.

eNeuro

Research Article: New Research | Sensory and Motor Systems

Impact of NMDA Receptor Overexpression on Cerebellar Purkinje Cell Activity and Motor Learning

Elisa Galliano[1], Martijn Schonewille[1], Saša Peter[1,2], Mandy Rutteman[1], Simone Houtman[1], Dick Jaarsma[1], Freek E. Hoebeek[1] and Chris I. De Zeeuw[1,2]

[1]*Department of Neuroscience, Erasmus Medical Centre, Rotterdam, the Netherlands*

[2]*Netherlands Institute for Neuroscience, Royal Netherlands Academy of Arts & Sciences, Amsterdam, the Netherlands*

DOI: 10.1523/ENEURO.0270-17.2018

Received: 2 August 2017

Revised: 24 December 2017

Accepted: 23 January 2018

Published: 29 January 2018

Funding: Dutch Organization for Medical Science

Funding: Erasmus University Fellowship

Funding: http://doi.org/10.13039/501100000780European Commission (EC)

Funding: http://doi.org/10.13039/100010269Wellcome

Conflict of Interest: Authors report no conflict of interest.

Authors' contributions: SH generated the mouse model. EG, MR and DJ designed, performed and analyzed the molecular and morphological experiments. EG, SP, MR, FEH and CIDZ. designed, performed and analyzed the in vitro electrophysiological experiments. EG, MS and CIDZ. designed, performed and analyzed the behavioral experiments. EG, DJ, FEH and CIDZ guided the project. EG, MS, FEH and CIDZ co-wrote the manuscript.

This work was supported by the Dutch Organization for Medical Sciences (ZonMw; FEH and CIDZ), Life Sciences (ALW; MS, FEH and CIDZ), Erasmus University Fellowship (MS and FEH), Senter (Neuro-Bsik) and ERC-adv of the European Community (CIDZ). EG is currently supported by a Sir Henry Wellcome Postdoctoral Fellowship.

Present address: Elisa Galliano, Centre for Developmental Neurobiology, King's College London, UK and Department of Molecular and Cellular Biology, Harvard University, USA.

*E.G. and M.S. contributed equally to this work.

Correspondence should be addressed to either Elisa Galliano, Centre for Developmental Neurobiology, King's College London, SE1 1UL London, United Kingdom or Department of Molecular and Cellular Biology, Harvard University, MA 20139 Cambridge, USA. E-mail: elisa.galliano@kcl.ac.Uk or Chris De Zeeuw, Department of Neuroscience, Erasmus Medical Centre, 3015 GE Rotterdam, The Netherlands. E-mail: c.dezeeuw@erasmusmc.nl

Cite as: eNeuro 2018; 10.1523/ENEURO.0270-17.2018

Alerts: Sign up at eneuro.org/alerts to receive customized email alerts when the fully formatted version of this article is published.

Accepted manuscripts are peer-reviewed but have not been through the copyediting, formatting, or proofreading process.

Copyright © 2018 Galliano et al.
This is an open-access article distributed under the terms of the Creative Commons Attribution 4.0 International license, which permits unrestricted use, distribution and reproduction in any medium provided that the original work is properly attributed.

eNeuro Accepted Manuscript

eNeuro Accepted Manuscript

Impact of NMDA receptor overexpression on cerebellar Purkinje cell activity and motor learning

Abbreviated title: NMDAR overexpression in Purkinje cells

Elisa Galliano[1,¥,*], Martijn Schonewille[1,*], Saša Peter[1,2], Mandy Rutteman[1], Simone Houtman[1], Dick Jaarsma[1], Freek E. Hoebeek[1] and Chris I. De Zeeuw[1,2]

1. Dept. of Neuroscience, Erasmus Medical Centre, Rotterdam, The Netherlands
2. Netherlands Institute for Neuroscience, Royal Netherlands Academy of Arts & Sciences, Amsterdam, The Netherlands

¥ Current address: Centre for Developmental Neurobiology, King's College London, UK and Department of Molecular and Cellular Biology, Harvard University, USA

* These authors contributed equally

Authors' contributions

SH generated the mouse model. EG, MR and DJ designed, performed and analyzed the molecular and morphological experiments. EG, SP, MR, FEH and CIDZ. designed, performed and analyzed the *in vitro* electrophysiological experiments. EG, MS and CIDZ. designed, performed and analyzed the behavioral experiments. EG, DJ, FEH and CIDZ guided the project. EG, MS, FEH and CIDZ co-wrote the manuscript.

Correspondence should be addressed to EG or CIDZ

- Elisa Galliano, Centre for Developmental Neurobiology, King's College London, SE1 1UL London, United Kingdom or Department of Molecular and Cellular Biology, Harvard University, MA 20139 Cambridge, USA ; elisa.galliano@kcl.ac.uk
- Chris De Zeeuw, Department of Neuroscience, Erasmus Medical Centre, 3015 GE Rotterdam, The Netherlands; c.dezeeuw@erasmusmc.nl

Numbers

Figures 4, tables 1, multimedia 0.

Number of words: abstract 146, significance statement 120, introduction 710, discussion 869

Acknowledgments

We are grateful to Y. Elgersma for supervision and advice in generating the transgenic lines; E. Haasdijk, R. de Avila Freire, C. Bruinsma and D. Groeneveld for technical assistance; Z. Nusser (Budapest) for advice on NMDAR immunohistochemistry; D. Rizopoulos for advice on the statistics analysis; B. van Beugen and Z. Gao for critical discussions.

Conflict of interest: none

Funding sources

This work was supported by the Dutch Organization for Medical Sciences (ZonMw; FEH and CIDZ), Life Sciences (ALW; MS, FEH and CIDZ), Erasmus University Fellowship (MS and FEH), Senter (Neuro-Bsik) and ERC-adv of the European Community (CIDZ). EG is currently supported by a Sir Henry Wellcome Postdoctoral Fellowship.

eNeuro Accepted Manuscript

Abstract

In many brain regions involved in learning *N*-methyl-D-aspartate glutamate receptors (NMDARs) act as coincidence detectors of pre- and post-synaptic activity, mediating Hebbian plasticity. Intriguingly, the parallel fiber (PF) to Purkinje cell (PC) input, which is critical for procedural learning, shows virtually no postsynaptic NMDARs. Why is this? Here, we address this question by generating and testing independent transgenic lines that over-express NMDA-NR2B specifically in PCs. PCs of the mice that show larger NMDA-mediated currents than controls at their parallel fiber (PF) input, suffer from a blockage of long-term potentiation (LTP) at their PF-PC synapses, while long-term depression (LTD) and baseline transmission are unaffected. Moreover, introducing NMDA-mediated currents affects cerebellar learning in that phase-reversal of the vestibulo-ocular reflex is impaired. Our results suggest that under physiological circumstances PC spines lack NMDARs postsynaptically at their PF input so as to allow LTP to contribute to motor learning.

Significance statement

NMDA-receptors form one of the key molecules involved in memory formation, yet they are absent in one of the most plastic synapses in the brain, the parallel fiber (PF) to Purkinje cell (PC) synapse. PCs are equipped with the molecular machinery for expression of NMDA-receptors, but under normal conditions all NMDA-receptors are directed towards their climbing fiber input. So why are NMDA-receptors not occurring postsynaptically at their PF input, which is known as the main substrate of cerebellar plasticity? To answer this question we generated two transgenic mouse lines that overexpress NMDA-receptors at the PF-PC synapse, and we show that while such manipulation does not result in abnormal morphology or baseline PC electrophysiology, it does impact plasticity and motor learning.

eNeuro Accepted Manuscript

Introduction

A basic property of chemical synapses is their ability to be permanently modified in response to stimulus patterns. This property, which is known as long-term synaptic plasticity, can result in potentiation or depression of transmission, and is thought to serve as a cellular basis for memory formation (Bliss and Lomo, 1973). The existence of long-term synaptic plasticity was predicted by Donald Hebb, who postulated that the synaptic connection between two neurons would be strengthened when pre- and postsynaptic elements are active simultaneously (Hebb, 1949). Such a process implies the existence of a coincidence detector able to sense at the same time the pre- and postsynaptic activity. The *N*-methyl-D-aspartate receptor (NMDAR), which is a cationic channel sensitive for glutamate released at the presynaptic site and voltage changes at the postsynaptic site, is a well-known coincidence detector, the activity of which appears to be key to the induction of various types of synaptic plasticity in the CNS (Cotman et al., 1988). However, in the cerebellar Purkinje cell (PC), a neuron with great capacity for synaptic plasticity (Carey, 2011; Gao et al., 2012), things are peculiar. First, NMDARs in PCs are expressed relatively late, after the second postnatal week; second, their NMDARs are expressed at a relatively low level; and finally, NMDAR currents in PCs can only be measured at just one of their inputs, *i.e.* the climbing fiber (CF) synapse (Piochon et al., 2007; Renzi et al., 2007), where they are required for the induction of long-term depression at the parallel fiber to Purkinje cell synapse (PF-PC LTD) (Piochon et al., 2010). So why are there virtually no functional NMDARs postsynaptically at the other glutamatergic afferent to PCs, *i.e.* the PF synapse? This is an intriguing question, especially given the facts that PF to PC synapses are abundant (between 100,000 and 200,000 for each PC),

eNeuro Accepted Manuscript

105 that these synapses show multiple forms of plasticity, and that they even express
106 NMDARs presynaptically (Bidoret et al., 2009; Bouvier et al., 2016). One could
107 speculate that since the opening of NMDARs will induce a calcium influx (Nicoll and
108 Malenka, 1995), and the level of calcium influx in turn will determine to what extent a
109 PF-PC synapse will be potentiated or depressed at its postsynaptic site (Coesmans
110 et al., 2004), it is possible that the virtual absence of NMDARs at this synapse is
111 necessary to keep the local calcium transients at PC spines relatively low and
112 thereby allow long-term potentiation (LTP) to occur. Here, we set out to test the
113 hypothesis that the lack of NMDARs at the PF-PC synapse is permissive for LTP
114 induction by generating novel Purkinje cell specific transgenic mouse lines that over-
115 express the NR2B subunit of NMDARs under the L7-promotor (L7-NR2B+/Tg1 and
116 L7-NR2B+/Tg2; hereafter referred to as Tg1 and Tg2) and by subsequently
117 investigating their cellular and behavioral consequences. We selected the form B of
118 the NR2 subunit, because this is the most permeable subunit for Ca^{2+}, it has been
119 shown to enhance synaptic plasticity, it is not expressed by any other neuron in the
120 cerebellar cortex, and it has previously been inserted successfully in neuronal
121 cultures, forming functional units with NR1 (Feldmeyer and Cull-Candy, 1996;
122 Kakegawa et al., 2003; Monyer et al., 1994). To minimize the possibility that all new
123 overexpressed NMDARs would be directed to the climbing fiber synapse as occurs
124 under physiological circumstances (Piochon et al., 2007; Renzi et al., 2007), we
125 overexpressed NR2B subunits with truncated UTR sites, which might serve as
126 regulatory elements for subcellular trafficking (Di Liegro et al., 2014; Wood et al.,
127 1996). Our data show that such overexpression of NR2B subunits in PCs *in vivo*
128 results in functional NMDARs and that many of the genetically induced, additional
129 NMDA-mediated currents are located at the PF to PC synapse. Moreover,

eNeuro Accepted Manuscript

overexpression of NR2B impaired induction of LTP, but not LTD, at the PF to PC synapse, and affected adaptation of the vestibulo-ocular reflex (VOR), which is known to depend on LTP (De Zeeuw and Ten Brinke, 2015; Gutierrez-Castellanos et al., 2017; Schonewille et al., 2010; Voges et al., 2017). Together, these findings highlight the quintessence of regulating the low and site-specific expression of NMDAR subunits in PCs, setting it apart from that in other neurons involved in memory formation (Kessels et al., 2013; Nabavi et al., 2013).

eNeuro Accepted Manuscript

Methods

Generation of transgenic mice

The NR2B transgene (Mouse Grin2b-001; ENSMUST00000053880.12) including 470 bases of the 3' UTR, was cloned into expression vector pGEM-L7containing the L7-promoter (Barski et al., 2000), by fusing the ATG initiation codon of the NR2B transgene with the initiation codon of the L7 gene. The resulting pGEM-L7NR2B was digested with with SalI/ClaI and the insert was used to generate the transgenic founders by pronuclear injection into C57BL/6NHsd inbred zygotes. The inbred founders were crossed into C57BL/6NHsd to produce F1 generation, two of which were selected for F2 offspring (Tg1 and Tg2) against a C57BL/6NHsd background. The genotypes of all offspring were analyzed by preparing tail DNAs. The 5' and 3' primers for detecting NR2B transgene were L7 S (CAC TTC TGA CTT GCA CTT TCC TTG G), L7 AS (TTC TTC AAG CTG CCC AGC AGA GCT C) and 165 (GCC AAA CTG GAA GAA CAT GGA GGA C); wild-type 450 bp, transgenic 557 bp. Mouse tail DNAs (about 1 mg) were amplified (94°C 3'//94°C 1'; 58°C 45"; 72°C 1':30cycles//72°C 10'// 4°C) on a Robo cycler. For all experiments the researchers were blind to the genotype of the animals. Unless stated otherwise we used 6 ± 1 weeks old male and female littermates, gender-matched across groups. All experiments were performed in accordance with the guidelines for animal experiments of Erasmus MC, Netherlands Institute for Neuroscience (KNAW), and the Dutch National Legislation.

Western Blot

Lysates for Western Blot were prepared by quick dissection of the brain and by homogenization of the brain tissue in lysis buffer (10 mM TRISHCl 6.8, 2.5% SDS, 2

eNeuro Accepted Manuscript

mM EDTA) and protease and phosphatase inhibitor cocktails (Sigma). The concentration of the lysates was adjusted to 1 mg/ml and a 10 µg volume was used for Western blot analysis. Western blots were probed with antibodies directed against the N-terminal NR2B (anti-mouse, 1:1000; Cell Signaling) and NR1 (anti-rabbit, 1:1000; Cell Signaling). Bands were visualized using Enhanced Chemo Luminescence (Pierce). Loading controls were performed with anti-actin antibodies (1:20000, Cell Signaling).

Histology

Mice were anesthetized with an overdose of Nembutal (i.p.) and transcardially perfused with saline followed by 4% paraformaldehyde (in 0.12 M phosphate buffer; PB). Sagittal sections (40-µm thick) were processed free-floating for calbindin immunohistochemisty or NR2B-immunofluoresence. For NR2B-immunofluoresence sections were exposed to limited proteolytic digestion to expose synaptic receptors (Watanabe et al., 1998): Sections were incubated in 0.2 M HCl containing 0.4 mg／mL pepsin (Sigma) for 20 min with continuous agitation. After rinsing in PBS and pre-incubation with PBS with 0.1% Triton X-100 (PBST) and 10% normal horse serum, the sections were incubated in PBST/1% normal horse serum with Ms anti-NR2B (NeuroMab clone N59/36; dilution 1:1000) for 48 h at 4 °C. NR2B antibody was visualized with Cy3-Donkey anti-mouse secondary antibody (1:400), and analyzed with (Zeiss Jena, Germany) LSM 700 upright confocal laser scanning microscope. For calbindin immunohistochemistry, after preincubation in PBST sections were incubated with Rabbit anti-Calbindin (Swant; dilution 1:15000) in PBST/1% normal horse serum for 48 h at 4 °C, followed by incubation with biotinylated goat-anti-rabbit secondary antibody (1:200; Vector), incubation with avidin-biotin-peroxidase complex

eNeuro Accepted Manuscript

189 (ABC) (Vector Laboratories, Burlingame, CA, USA), and reaction with
190 diaminobenzidine (DAB, 0.05%). Calbindin-immunoperoxidase-stained sections were
191 analyzed using a Leica (Nussloch, Germany) DM-RB microscope, or scanned with a
192 Hamamatsu NanoZoomer 2 whole slide imager and analyzed with NDP.view
193 (Hamamatsu city, Japan) software. For Golgi staining, which was used for Sholl
194 analysis, Tg1-, Tg2- and control mice were perfused with saline, followed by a
195 buffered aldehyde fixative and a mordant consisting of 6% potassium dichromate, 6%
196 chloral hydrate, and 4% formaldehyde. After postfixation in the same mordant for 3
197 days, blocks of the cerebellar cortex were treated with 0.75% silver nitrate for an
198 additional 3 days, embedded in a soft Epon mixture and sectioned with a heated
199 steel knife (De Zeeuw et al., 1996).
200
201 ***In vitro* electrophysiology**
202
203 Mice (6±1 weeks old) were decapitated under isoflurane anaesthesia. Subsequently,
204 the cerebellum was removed and transferred into ice-cold slicing medium containing
205 (in mM): 240 Sucrose, 5 KCl, 1.25 Na_2HPO_4, 2 $MgSO_4$, 1 $CaCl_2$, 26 $NaHCO_3$ and 10
206 D-Glucose, bubbled with 95% O_2 and 5% CO_2. Parasagittal slices (200- or 250-µm
207 thick) of the cerebellar vermis were cut using a vibratome (VT1000S, Leica) and
208 afterwards kept in ACSF containing (in mM): 124 NaCl, 5 KCl, 1.25 Na_2HPO4, 2
209 $MgSO_4$, 2 $CaCl_2$, 26 $NaHCO_3$ and 20 D-Glucose, bubbled with 95% O_2 and 5% CO_2
210 for > 1 h before the experiments started. *In vitro* experiments were performed in
211 slices at room temperature (20-22 °C), which were continuously perfused with ACSF
212 that was supplemented with picrotoxin (100µM) or bicuculline methiodide (20µM) to
213 block $GABA_A$ receptors. All drugs were purchased from Sigma (St. Louis, MO).

eNeuro Accepted Manuscript

Whole-cell patch-clamp recordings were performed using either an EPC-10 amplifier (HEKA Electronics, Lambrecht, Germany) or an Axopatch amplifier 700B (Molecular Devices, Union City, CA, USA). PCs were visualized using an upright microscope (Axioskop 2 FS plus, Carl Zeiss, Jena, Germany) equipped with a 40X water immersed objective. If not stated otherwise, recording electrodes were filled with an intracellular solution containing (in mM): 124 K-Gluconate, 9 KCl, 10 KOH, 4 NaCl, 10 HEPES, 28.5 Sucrose, 4 Na_2ATP, 0.4 Na_3GTP (pH 7.25-7.35; osmolarity ~290). For extracellular stimulation, patch electrodes filled with ACSF were positioned to touch the surface of the slice at the most distal 1/3 of the molecular layer lateral to the recorded PCs for PF stimulation and in the granular layer close to the recorded PC for CF stimulation. Recordings were excluded if series or input resistances (R_S and R_I, respectively) (assessed by -10 mV voltage steps following each test pulse) varied by > 15% over the course of the experiment. The liquid junction potential was not corrected for. Quantification of NMDA currents was performed in magnesium-free ACSF supplemented with glycine (10 µM, Sigma) by subsequent application of the AMPA antagonist NBQX (12.5 µM, Tocris) and the NMDA antagonist D-AP5 (10 µM, Tocris). All-or-none climbing fibers responses were first identified in current clamp by the typical complex spike shape and the absolute NMDA contribution was calculated in voltage clamp (holding potential -65 mV) by subtracting the NBQX+AP5 insensitive residual component to the NBQX sensitive. PF responses of approximately -200 pA were taken as a baseline in voltage clamp (holding potential -65 mV) and the NMDA contribution was calculated as described for CF-responses but normalized to the baseline response. Rs was compensated online to obtain a residual value > 10 MΩ. PC intrinsic excitability was recorded in current-clamp mode at 34 ± 1 °C. PCs were discarded when >800 pA hyperpolarizing current was required to maintain the

eNeuro Accepted Manuscript

239 holding potential at -65 mV or when action potential firing occurred at this holding
240 potential. We injected 800 ms current steps ranging from -100 to +1000 pA with 100
241 pA increments. The average spiking frequency measured over the entire current
242 pulse was used to construct current-frequency plots. Action potential properties (peak
243 amplitude, after-hyperpolarization amplitude and half-width) were evaluated using the
244 first action potential generated by each PC. To assess the stimulus intensity - EPSC
245 amplitude (input-output) ratio consistently, only PCs were selected in regions with
246 comparable width of the molecular layer. For these recordings electrodes contained
247 (in mM): 130 $CsMeSO_4$, 4 $MgCl_2$, 0.2 EGTA, 10 HEPES, 10 Na-Phosphocreatine, 1
248 QX-314, 4 Na_2ATP, 0.4 Na_3GTP (pH 7.25-7.35). LTP at the PF-PC synapse was
249 assessed by PF stimulation at 1 Hz for 5 min (PF-LTP protocol; Coesmans et al.,
250 2004), while long-term depression (LTD) was induced by PF activation (10 stimuli at
251 100 Hz) and CF activation (2 stimuli at 20 Hz), repeated 30 times every 10 s at 34 ±
252 1°C (PF-LTD protocol; (Safo and Regehr, 2005). Test responses were evoked at a
253 frequency of 0.05 Hz (2 stimuli of 0.5-6 µA pulses; 50 ms inter-stimulus interval). PCs
254 were clamped at -65 to -70 mV to prevent spontaneous action potential firing.
255 Plasticity of PC's intrinsic excitability was recorded in current-clamp mode at 34 ±
256 1°C. PCs were discarded when >800 pA hyperpolarizing current was required to
257 maintain the holding potential at -65 mV or when action potential firing occurred at
258 this holding potential. We induced intrinsic plasticity by 1 Hz PF stimulation for 5 min
259 (PF-LTP protocol, comparable to Belmeneguai et al, 2010, but with short ramping
260 current injections to probe the response; see Fig. 3D) at I=0. Four current steps (800
261 ms), ranging from 100 to 800 pA in 100 pA increments were injected to evoke action
262 potential firing during steps 2-4. The spike count at the third current step was taken
263 as a measure of excitability. RI was calculated from the first hyperpolarizing current

eNeuro Accepted Manuscript

264 injection. To determine if plasticity was induced a linear mixed model was used
265 based on dividing the post-tetanus period into two 15 min periods (post1 and post2)
266 and comparing these to pre-tetanus values (pre). For LTP, LTD, and intrinsic
267 plasticity (IP) the estimates of fixed effects (of tetanus stimulus) on EPSCs in control
268 mice were: LTP, post1 vs pre, estimated +25.9 ± 4.9 %, $p < 0.001$; post2 vs. pre,
269 estimated +21.3 ± 5.0 %, $p < 0.001$; LTD, post1 vs pre, estimated –21.7 ± 5.5 %, $p <$
270 0.001; post2 vs. pre, estimated –12.8 ± 5.6 %, $p = 0.022$; LTP with D-AP5, post1 vs
271 pre, estimated +10.2 ± 1.9 %, $p < 0.001$; post2 vs. pre, estimated +6.9 ± 1.9 %, $p <$
272 0.001; and IP, post1 vs pre, estimated –4.3 ± 4.5 %, $p =0.34$; and post2 vs. pre,
273 estimated +16.1 ± 4.6 %, $p = 0.001$. To compare genotypes a repeated measures
274 ANOVA was used on the 20 min recording period post tetanus (the minimal recording
275 duration).
276
277 **Open field**
278 To test locomotor activity and anxiety, individual mice were placed in a circular,
279 dimly–lit open field (120 cm diameter), and the total distance traveled, together with
280 the average speed of each mouse, was recorded for 10 min (SMART software,
281 Panlab, Barcelona, Spain).
282
283 **Compensatory eye movements**
284 During their fifth postnatal week mice were prepared for chronic, head-restrained
285 recordings of compensatory eye movements. Mice were 37 ± 3 days at the beginning
286 of the 5 days of compensatory eye movement testing. In short, under isoflurane
287 anaesthesia (initiation at 4%, maintenance at ~1.5% with O_2) a pedestal was
288 constructed using Optibond primer and adhesive (Kerr, Bioggio, Switzerland) and

eNeuro Accepted Manuscript

Charisma (Haeraeus Kulzer, Armonk, NY, USA). After a recovery period (2-3 days) mice were head-fixed by means of a magnet (Neodymium, 4x4x2 mm, MTG Europe, Weilbach, Germany) embedded in a custom-made U-shaped pedestal and a securing screw. A cylindrical screen (diameter 63 cm) with a random-dotted pattern (each element 2°) surrounded the turntable (diameter 60 cm) on which the mouse was placed. The optokinetic reflex (OKR) and the vestibulo-ocular reflex in dark (VOR) and light (VVOR) were elicited by sinusoidal rotation of either drum (OKR) or table (VOR and VVOR). Motor performance was tested by rotating at 0.1-1.0 Hz with 5° amplitude (fixed). Each frequency – amplitude combination was tested twice with 8 (for 0.1 Hz) to 20 (for 1.0 Hz) repeated cycles and results were averaged. Motor learning was tested by mismatching visual and vestibular input: 'gain decrease' was evoked by rotating drum and table in phase at the same amplitude (5°) at 0.6 Hz and 'phase reversal' by subsequent rotation in phase with increased amplitude of the drum (day 2, 7.5°; day 3, 10°) at the same frequency. Animals were kept in the dark in between training sessions. Phase reversal results are depicted as gain multiplied by the cosine of the phase to capture the change in timing and amplitude of movement in a single value (gain*cos(phase). Phase values larger than 90° result in a negative gain*cos(phase) value. Consolidation was calculated as the learned response on the second day as a percentage of the learning during the first day; for example, gain decrease consolidation = $100\% \cdot (g_{max\text{-}day1} - g_{max\text{-}day2} / (g_{max\text{-}day1} - g_{min\text{-}day1})$, with $g_{min\text{-}day1}$ being the minimum gain on day 1 and $g_{max\text{-}day2}$ the maximum gain on day 2. To illuminate the eye during the recordings we used two table-fixed infrared emitters (OD-50L, max. output 600 mW, dispersion angle 7°, peak wavelength 880 nm; Opto-Diode, Camarillo, CA, USA), and a third emitter mounted to the camera aligned horizontally with the camera's optical axis. This third emitter produced the

eNeuro Accepted Manuscript

tracked corneal reflection. The pupil position, after subtraction of the corneal reflecting position, was recorded using the eye-tracking device (ETL-200, ISCAN systems, Burlington, NA, USA). Calibrations were performed as described previously (Stahl et al., 2000). Gain and phase values of the eye movements were calculated using a custom-made Matlab routine (Matlab, MathWorks Inc, Natick, Massachusetts, USA). Gain and phase results plotted against frequency or time were statistically analyzed using repeated-measures ANOVA.

Data analysis

All values are represented as mean ± SEM, *p*-values of < 0.05 were considered significant. Data distributions were evaluated using either Levene's test of equality of variance for independent data or Mauchly's test of sphericity for repeated measures. Unless stated otherwise, statistical analysis was done using one-way ANOVA test with Tukey's post-hoc correction where three groups were compared (see Table for details per test).

eNeuro Accepted Manuscript

331

332 **Table 1: Statistical testing**

Figure	Data	Data Structure	Type of test	Actual power
2A	CF to PC NMDA current	normal distr.	One-way ANOVA	0.988
2B	PF to PC NMDA current	Non-normal distr.	Kruskal-Wallis Test	0.940
2C	I-O Linear fit slope	normal distr.	One-way ANOVA	0.295
	I-O First spike peak amplitude	normal distr.	One-way ANOVA	0.369
	I-O First spike AHP amplitude	normal distr.	One-way ANOVA	0.769
	I-O First spike half-width	normal distr.	One-way ANOVA	0.319
2D	slope EPSC I-O	normal distr.	Rep. measures ANOVA	0.077
3A	PF-PC LTP group comparison	normal distr.	Rep. measures ANOVA	0.592
3B	PF-PC LTD group comparison	normal distr.	Rep. measures ANOVA	0.079
3C	PF-PC LTP with D-AP5 - groups	normal distr.	Rep. measures ANOVA	0.057
3D	Intrinsic plasticity - 10min	normal distr.	Rep. measures ANOVA	0.589
3D	Intrinsic plasticity - 20min	normal distr.	Rep. measures ANOVA	0.386
4A	open field - path length	normal distr.	Two-sample t-test	0.283
	open field - average speed	normal distr.	Two-sample t-test	0.280
4B	OKR - gain	normal distr.	Rep. measures ANOVA	0.071
	OKR - phase	normal distr.	Rep. measures ANOVA	0.086
4C	VOR - gain	normal distr.	Rep. measures ANOVA	0.136
	VOR - phase	normal distr.	Rep. measures ANOVA	0.314
4D	VVOR - gain	normal distr.	Rep. measures ANOVA	0.191
	VVOR - phase	normal distr.	Rep. measures ANOVA	0.105
4E	VOR gain decrease training	normal distr.	Rep. measures ANOVA	0.157
	VOR gain decr consolidation	normal distr.	Two-sample t-test	0.329
4F	VOR gain*phase reversal day 2	normal distr.	Rep. measures ANOVA	0.050
	VOR gain*phase reversal day 3	normal distr.	Rep. measures ANOVA	0.862
	VOR gain*phase reversal day 4	normal distr.	Rep. measures ANOVA	0.635
	VOR gain*phase reversal day 5	normal distr.	Rep. measures ANOVA	0.948

333
334

335

eNeuro Accepted Manuscript

Results

Transgenic overexpression of NR2B in PCs increases climbing fiber to PC NMDA responses and introduces functional NMDA receptors in parallel fiber to PC synapses

NMDA receptors are complex, heterotetrameric channels formed by two NR1 subunits and two NR2 subunits (Tovar and Westbrook, 2017). Under normal developmental and physiological circumstances NR1 is expressed by PCs directly after birth, while NR2 subunits, required to form functional receptors at the climbing fiber to PC synapses, are not expressed until 2 to 3 weeks after birth, reaching a plateau at approximately 2 months (Piochon et al., 2007) (Figure 1A). To introduce functional NR1/NR2 NMDA currents at the parallel fiber to PC synapse, we generated transgenic mouse lines over-expressing the NR2B subunit by inserting the linearized NR2B transgene without its 5'-UTR and most of its 3'-UTR (leaving only 470 bases) under control of the Pcp-2/L7 promoter in an expression vector (Barski et al., 2000; De Zeeuw et al., 1998), which was pronuclearly injected into a C57BL/6 inbred zygote (see methods for detailed procedures). Western blot analysis at six weeks of age confirmed the over-expression of NR2B protein in the cerebellum of two lines of L7-NR2B+ transgenic animals, Tg1 and Tg2 (Figure 1B). In accord with increased expression of NR2B in Purkinje cells, immuno-fluorescence showed increased NR2B staining in the cerebellar molecular layer of both transgenic lines (Figure 1C). Western blot and immunohistology also indicated that in both transgenic lines labeling in the cerebellum was still considerably lower than that in hippocampus and cortex, which are known for very high levels of NR2B expression (Monyer et al., 1994). The ratio of NR-labeling to loading control actin labeling indicated a relatively

eNeuro Accepted Manuscript

high amount of the actual protein present in Tg2, but the generally low expression levels and suboptimal antibody quality, commonly seen with channel receptors, prohibited an accurate evaluation of the sub-cellular localization or quantification of the expression. We therefore took these results as qualitative evidence for the presence of NR2B, while the functional consequences and related quantifications were tested with cell physiological approaches (see below).

Both Tg1 and Tg2 mice showed normal growth, body weights and breeding ratios compared to control littermates. The cyto-architecture of the cerebellum of both lines was normal and their foliation was well preserved (Figure 1D). Immunohistochemistry for calbindin-D28K and Sholl analysis of Golgi material of the mice indicated that morphology of Purkinje cells was unaltered (Figure 1E). Furthermore, behavior of both Tg1 and Tg2 in the home cage was indistinguishable from that of wild-type littermates.

To determine whether ectopic NR2B subunits assemble and result in altered synaptic NMDA currents in PCs, we performed patch-clamp recordings of PCs in acute cerebellar slices bathed in Mg^{2+}-free solution with subsequent application of AMPAR and NMDAR blockers (NBQX and D-AP5, respectively). In line with previous studies (Piochon et al., 2007; Renzi et al., 2007), PCs from 6-week old controls showed a NMDA-mediated current (*i.e.* NBQX-insensitive and AP5-sensitive) at the CF to PC synapse (77 ± 21 pA). In both Tg1 and Tg2 mutant mice the NMDAR-mediated currents at CF-PC synapses were significantly larger than those in controls (262 ± 52 and 365 ± 41 pA; $p = 0.025$ and $p = 0.001$ vs. Ctrl, respectively) (Figure 2A). Next, we determined whether NMDA-mediated currents also occurred at the PF to PC synapse; *i.e*. we quantified the percentage of a 200-300 pA PF to PC excitatory postsynaptic current (EPSC) that was NMDA-mediated. These percentages were

eNeuro Accepted Manuscript

386 negligible in controls (4 ± 1 %), modestly present in Tg1 (18 ± 5 %), but more
387 prominently present in Tg2 PCs (38 ± 11 %); the percentage of Tg2, but not that of
388 Tg1, was significantly higher than that in controls (p = 0.001 and p = 0.10,
389 respectively) (Figure 2B).

390 Next to study the effect of ectopic NR2B expression on basic PC
391 electrophysiological properties we first performed whole cell current-clamp recordings
392 at physiologically relevant temperatures to investigate intrinsic excitability (Figure
393 2C). PCs of all genotypes showed increasing action potential firing frequencies upon
394 somatic current injections of increasing amplitude comparable to the ones of their
395 control littermates. The slope of the linear input-output relationship in transgenic mice
396 did not differ from that in control animals (Tg1 17.4 ± 1.5 Hz/pA, Tg2 18.1 ± 1.9
397 Hz/pA, Ctrls 15.0 ± 0.9 Hz/pA; p = 0.47 and p = 0.45 for Tg1 and Tg2 vs. Ctrls,
398 respectively), indicating a normal level of excitability. In addition, for each cell we
399 analyzed the action potential properties and again we found no significant differences
400 in terms of spike baseline, peak amplitude, after-hyperpolarization amplitude or half-
401 width among genotypes (all p values > 0.13). Finally, the presence of NMDARs in
402 PCs prompted us to investigate the post-synaptic amplitude evoked by PF stimulation
403 (*i.e.* in a recording solution with Mg^{2+} and holding at -65 mV) at increasing stimulus
404 intensities (Figure 2D). No obvious differences were found in the EPSC kinetics (all
405 p-values > 0.9), nor in the input/output ratio of PF-EPSCs between transgenic
406 animals and controls (p = 0.83, repeated measures ANOVA).

407 Taken together, our data show that we generated transgenic mice over-
408 expressing NR2B subunits without affecting baseline transmission, but that only Tg2
409 showed significantly more NMDAR-mediated currents at their PF to PC synaptic
410 inputs compared to Ctrls.

eNeuro Accepted Manuscript

411

412 **NMDA currents at the PF-PC synapse selectively prevent the induction of long-**
413 **term potentiation**

414 While induction of PF to PC LTD depends on CF activation for its high Ca^{2+} influx,
415 LTP is achieved through repetitive stimulation of only PFs and requires a low Ca^{2+}
416 concentration (Coesmans et al., 2004) and has been shown to be independent of
417 postsynaptic NMDARs (Piochon et al., 2010) (Wang et al., 2014). We therefore
418 hypothesized that insertion of Ca^{2+}-permeable NMDARs at the PF-PC synapse would
419 affect LTP induction (Figure 3A). Given that only Tg2 showed significantly more
420 NMDA-mediated currents at their PF-PC synapses than controls, we focused our
421 plasticity experiments on Tg2 and their wild type littermates. Indeed, whereas the
422 controls showed normal potentiation (pre- vs. post-tetanus: $p < 0.001$, Linear Mixed
423 Model, see Methods), the amplitude of the EPSCs of the Tg2 mice after LTP
424 induction was significantly lower from the ones recorded in control cells (Tg2 vs. Ctrls
425 $p = 0.034$, repeated measures ANOVA). In contrast, LTD at the PF to PC synapse
426 (Ctrls, pre- vs. post-tetanus: $p < 0.05$, Linear Mixed Model, see Methods) was not
427 affected (Tg2 vs. Ctrls, $p = 0.63$, repeated measures ANOVA) (Figure 3B). To
428 unequivocally link the phenotype in LTP induction to the activation of NMDARs we
429 repeated the experiment in presence of NMDAR antagonist D-AP5 (Figure 3C).
430 Blocking NMDA currents minimized the effects on the induction of LTP (pre- vs. post-
431 tetanus for Ctrls, $p < 0.001$; Linear Mixed Model, see Methods), ablating the
432 difference between genotypes ($p = 0.80$, repeated measures ANOVA).

433 Impairment in PF to PC LTP induction often co-occurs with long-term deficits
434 in intrinsic plasticity (Belmeguenai et al., 2010; Peter et al., 2016; Schonewille et al.,
435 2010). Instead, in PCs of Tg2 mice the overall intrinsic plasticity was enhanced

eNeuro Accepted Manuscript

436 shortly after induction (p = 0.036 for the first 10 min after induction, 0.095 for the
437 entire period, repeated measures ANOVA) (Figure 3D). We conclude that over-
438 expression of NMDAR's in PCs selectively prevents the induction of LTP at the PF-
439 PC synapse, and that this deficit might be partly compensated for by a modest early
440 increase in intrinsic plasticity.
441
442 **Normal motor behavior but impairment in motor learning**
443 LTP at the PF-PC synapse probably does not affect baseline motor performance, but
444 it may well contribute to vestibulo-cerebellar motor learning (De Zeeuw et al., 2011;
445 Gao et al., 2012; Ito, 2002). At the same time, it should be noted that short-lasting
446 enhanced intrinsic plasticity, as observed in the Tg2 mutant, might partly compensate
447 for a deficit in LTP induction (De Zeeuw et al., 2011; Gao et al., 2012). To evaluate
448 the behavioral consequences of overexpression of NR2B in the Purkinje cells of the
449 Tg2 mice we subjected them to both motor performance and learning tests. First, we
450 confirmed that the general motor behavior of Tg2 animals was comparable to that of
451 their control littermates in an open field test; neither path length nor average speed
452 was affected (p = 0.28 and p = 0.29, respectively; Figure 4A). In addition, we
453 evaluated oculomotor activity, which is particularly sensitive to cerebellar deficits
454 (Boyden et al., 2006; Ito, 2002; Schonewille et al., 2010). Both gain and phase values
455 during the optokinetic reflex (OKR) as well as during the vestibulo-ocular reflex in the
456 dark (VOR) and the light (VVOR) elicited by sinusoidal stimulation at different
457 frequencies (0.1 – 1.0 Hz) with a fixed amplitude (5°) did not differ significantly
458 between genotypes (all p values > 0.13, repeated measures ANOVA; Figures 4B-D).
459 Next, we subjected the Tg2 animals to the type of VOR training that is most
460 sensitive, *i.e.* phase reversal learning, which is aimed at gradually converting the

eNeuro Accepted Manuscript

direction of the eye movements over several days of in-phase vestibular and visual stimulation (Badura et al., 2016). During the first session, which entails standard gain-decrease training evoked by rotating drum and table in-phase at 5° at 0.6 Hz, the amplitude of the VOR in Tg2 mice decreased to similar levels as that in control mice (p = 0.33, repeated measures ANOVA; Figure 4E).

Moreover, when the animals were tested again after spending 23 hours in the dark, the consolidation of the change in VOR gain was not different among genotypes (p = 0.21). However, when we subjected animals to phase reversal training for four consecutive days, the Tg2 mice performed worse than controls in that their adaptation was delayed. The training aims to reverse the direction of the VOR, resulting in a negative gain*cos(phase) value (Figure 4F) and this adaptation is impaired in Tg2 mouse from day 3 onwards (day 3, 4 and 5, p = 0.005, p = 0.026 and p = 0.001, respectively, repeated measures ANOVA). Together, these data show that NR2B transgenic mice have an unaffected baseline motor performance and that their learning capabilities are slightly, but significantly, affected.

eNeuro Accepted Manuscript

Discussion

To shed light on the surprisingly low expression level of the main coincidence detector in the brain, the NMDAR, we generated a transgenic mouse line that over-expresses NMDARs at one of the most studied and phylogenetically oldest sites of plasticity in the brain, the parallel fiber to Purkinje cell synapse. The L7-NR2B+ Tg2 mice, which expresses functional NMDAR-mediated currents not only at the CF-PC synapse, but also at the PF-PC synapse, develop normally and have no morphological abnormalities or impaired motor performance. Interestingly, the NMDAR-mediated currents diminish the ability for LTP induction at the PF-PC synapse and affects a demanding form of cerebellar-dependent motor learning, VOR phase-reversal learning.

As previously shown in an *in vitro* essay (Kakegawa et al., 2003), our data imply that NR1 subunits are sufficiently expressed in PCs to aggregate with the exogenously expressed NR2 subunits to form functional heterotetramers. As low expression levels and suboptimal antibody quality prohibit determining the sub-cellular localization of the NR2B subunit in our experiments, we cannot exclude the possibility of extra-synaptic receptors. The normal absence of NMDARs at PF input sites under physiological circumstances is therefore not caused by the scarceness of NR1 subunits, but by the limited and finely regulated NR2 expression and selective intracellular transport machinery (Piochon et al., 2007; Renzi et al., 2007), which may in part depend on the UTR sites of the subunits (Di Liegro et al., 2014; Wood et al., 1996). Moreover, it also appears that NMDARs are not absent from the PF-PC synapse in controls to prevent excitotoxicity (Slemmer et al., 2005), as we found no sign of PC death in our transgenic mouse lines. Still, the amount of NMDAR-

eNeuro Accepted Manuscript

501 mediated current was not massive, and we cannot exclude the possibility that higher
502 expression levels could potentially trigger PC apoptosis.

503 The main consequence of the genetically induced presence of NMDARs at the
504 PF-PC synapse is that it renders the synapse incapable of potentiation. In contrast to
505 other well-studied excitatory synapses, *e.g.* the well-characterized hippocampal CA3
506 to CA1 synapse or the synapses formed by the cerebellar mossy fibers with granule
507 cells and cerebellar nuclei neurons (Bliss and Lomo, 1973; D'Angelo et al., 1999;
508 Pugh and Raman, 2006), NMDARs at the PF-PC synapse are not only dispensable
509 for LTP induction, they are in fact effectively blocking it if present at the postsynaptic
510 site. The plasticity induction rule in PCs is, in terms of calcium dependence, reversed
511 compared to the traditional BCM-rule in pyramidal cells (Bienenstock et al., 1982;
512 Coesmans et al., 2004); hence, LTP induction is only possible when Ca^{2+}
513 concentrations are relatively low. In fact, in normal mice the presence or absence of
514 CF-triggered Ca2+-level increase determines the occurrence of LTD or LTP,
515 respectively, and this effect is independent of the change in Ca2+-level evoked by
516 the PF stimulation (Piochon et al., 2016). It is therefore tempting to hypothesize that
517 in our transgenic mice the presence of Ca^{2+}-permeable NMDARs increases the Ca^{2+}
518 concentration to a level that is too high to allow LTP, while leaving LTD induction
519 unaffected. Conversely, but in line with this concept, blocking Ca^{2+}-permeable
520 NMDARs in mature mice reduces the dendritic Ca^{2+} influx during a complex spike to
521 a level that is too low for LTD, while leaving LTP unaffected (Piochon et al., 2010).
522 Such a mechanism, which will have to be looked at in future studies, may also
523 explain why intrinsic plasticity was slightly increased in the Tg2 mice, as this form of
524 plasticity is largely regulated by the activity of SK2 channels, which is also Ca^{2+}-
525 dependent (Hosy et al., 2011; Maher and Westbrook, 2005). In this regard, the L7-

eNeuro Accepted Manuscript

NR2B+ Tg2 mice diverge from other LTP-deficient mutants in which the calcium dynamics are not directly affected. PC-specific mutants, such as the L7-PP2B-, L7-Shank2-, and L7-GluR3-mutants (Gutierrez-Castellanos et al., 2017; Peter et al., 2016; Schonewille et al., 2010), all do not only show a blockage of LTP induction, but they also show a profound reduction in intrinsic plasticity, rather than an enhancement as found here in the Tg2 mice. The combination of deficits in both LTP-induction and intrinsic plasticity leads to a more severe behavioral phenotype in that the VOR phase reversal adaptation is, unlike that of the Tg2 mice, virtually completely abolished (Gutierrez-Castellanos et al., 2017; Peter et al., 2016; Schonewille et al., 2010). Thus, the relatively mild behavioral phenotype of the Tg2 mice may be explained by an intact, if not elevated, level of intrinsic plasticity, which might also at least partly result from an elevated Ca^{2+}.

Our results fit with the interpretation that different types of plasticity in PCs – and in other cerebellar neurons – synergistically interact to ensure optimal learning (Gao et al., 2012). According to this theory, mutations that impair several plasticity mechanisms or network elements simultaneously typically affect more basic types of cerebellar-dependent learning and, if they do so, they affect them more severely (Galliano et al., 2013; Ichise et al., 2000; Schonewille et al., 2010; Wulff et al., 2009). In contrast, when a single mechanism at a single type of synapse in the circuit is impaired, other mechanisms may compensate (Gao et al., 2012) and the ability to perform and learn motor tasks may be maintained to a larger extent (this manuscript; (Schonewille et al., 2011).

eNeuro Accepted Manuscript

References

Badura, A., C. Clopath, M. Schonewille, and C.I. De Zeeuw. 2016. Modeled changes of cerebellar activity in mutant mice are predictive of their learning impairments. *Scientific reports*. 6:36131.

Barski, J.J., K. Dethleffsen, and M. Meyer. 2000. Cre recombinase expression in cerebellar Purkinje cells. *Genesis*. 28:93-98.

Belmeguenai, A., E. Hosy, F. Bengtsson, C.M. Pedroarena, C. Piochon, E. Teuling, Q. He, G. Ohtsuki, M.T. De Jeu, Y. Elgersma, C.I. De Zeeuw, H. Jorntell, and C. Hansel. 2010. Intrinsic plasticity complements long-term potentiation in parallel fiber input gain control in cerebellar Purkinje cells. *J Neurosci*. 30:13630-13643.

Bidoret, C., A. Ayon, B. Barbour, and M. Casado. 2009. Presynaptic NR2A-containing NMDA receptors implement a high-pass filter synaptic plasticity rule. *Proc Natl Acad Sci U S A*. 106:14126-14131.

Bienenstock, E.L., L.N. Cooper, and P.W. Munro. 1982. Theory for the development of neuron selectivity: orientation specificity and binocular interaction in visual cortex. *J Neurosci*. 2:32-48.

Bliss, T.V., and T. Lomo. 1973. Long-lasting potentiation of synaptic transmission in the dentate area of the anaesthetized rabbit following stimulation of the perforant path. *J Physiol*. 232:331-356.

Bouvier, G., D. Higgins, M. Spolidoro, D. Carrel, B. Mathieu, C. Lena, S. Dieudonne, B. Barbour, N. Brunel, and M. Casado. 2016. Burst-Dependent Bidirectional Plasticity in the Cerebellum Is Driven by Presynaptic NMDA Receptors. *Cell Rep*. 15:104-116.

Boyden, E.S., A. Katoh, J.L. Pyle, T.A. Chatila, R.W. Tsien, and J.L. Raymond. 2006. Selective engagement of plasticity mechanisms for motor memory storage. *Neuron*. 51:823-834.

Carey, M.R. 2011. Synaptic mechanisms of sensorimotor learning in the cerebellum. *Current opinion in neurobiology*. 21:609-615.

Coesmans, M., J.T. Weber, C.I. De Zeeuw, and C. Hansel. 2004. Bidirectional parallel fiber plasticity in the cerebellum under climbing fiber control. *Neuron*. 44:691-700.

Cotman, C.W., D.T. Monaghan, and A.H. Ganong. 1988. Excitatory amino acid neurotransmission: NMDA receptors and Hebb-type synaptic plasticity. *Annu Rev Neurosci*. 11:61-80.

D'Angelo, E., P. Rossi, S. Armano, and V. Taglietti. 1999. Evidence for NMDA and mGlu receptor-dependent long-term potentiation of mossy fiber-granule cell transmission in rat cerebellum. *J Neurophysiol*. 81:277-287.

De Zeeuw, C.I., C. Hansel, F. Bian, S.K. Koekkoek, A.M. van Alphen, D.J. Linden, and J. Oberdick. 1998. Expression of a protein kinase C inhibitor in Purkinje cells blocks cerebellar LTD and adaptation of the vestibulo-ocular reflex. *Neuron*. 20:495-508.

eNeuro Accepted Manuscript

589 De Zeeuw, C.I., F.E. Hoebeek, L.W. Bosman, M. Schonewille, L. Witter, and S.K. Koekkoek.
590 2011. Spatiotemporal firing patterns in the cerebellum. *Nat Rev Neurosci*. 12:327-344.

591 De Zeeuw, C.I., E.J. Lang, I. Sugihara, T.J. Ruigrok, L.M. Eisenman, E. Mugnaini, and R.
592 Llinas. 1996. Morphological correlates of bilateral synchrony in the rat cerebellar
593 cortex. *J Neurosci*. 16:3412-3426.

594 De Zeeuw, C.I., and M.M. Ten Brinke. 2015. Motor Learning and the Cerebellum. *Cold*
595 *Spring Harbor perspectives in biology*. 7:a021683.

596 Di Liegro, C.M., G. Schiera, and I. Di Liegro. 2014. Regulation of mRNA transport,
597 localization and translation in the nervous system of mammals (Review). *International*
598 *journal of molecular medicine*. 33:747-762.

599 Feldmeyer, D., and S. Cull-Candy. 1996. Functional consequences of changes in NMDA
600 receptor subunit expression during development. *Journal of neurocytology*. 25:857-
601 867.

602 Galliano, E., Z. Gao, M. Schonewille, B. Todorov, E. Simons, Andreea S. Pop, E. D Angelo,
603 Arn M.J.M. van den Maagdenberg, Freek E. Hoebeek, and Chris I. De Zeeuw. 2013.
604 Silencing the Majority of Cerebellar Granule Cells Uncovers Their Essential Role in
605 Motor Learning and Consolidation. *Cell Reports*.

606 Gao, Z., B.J. van Beugen, and C.I. De Zeeuw. 2012. Distributed synergistic plasticity and
607 cerebellar learning. *Nat Rev Neurosci*. 13:619-635.

608 Gutierrez-Castellanos, N., C.M. Da Silva-Matos, K. Zhou, C.B. Canto, M.C. Renner, L.M.
609 Koene, O. Ozyildirim, R. Sprengel, H.W. Kessels, and C.I. De Zeeuw. 2017. Motor
610 Learning Requires Purkinje Cell Synaptic Potentiation through Activation of AMPA-
611 Receptor Subunit GluA3. *Neuron*. 93:409-424.

612 Hebb, D.O. 1949. The organization of behavior. Wiley & Sons New York.

613 Hosy, E., C. Piochon, E. Teuling, L. Rinaldo, and C. Hansel. 2011. SK2 channel expression
614 and function in cerebellar Purkinje cells. *J Physiol*. 589:3433-3440.

615 Ichise, T., M. Kano, K. Hashimoto, D. Yanagihara, K. Nakao, R. Shigemoto, M. Katsuki, and
616 A. Aiba. 2000. mGluR1 in cerebellar Purkinje cells essential for long-term depression,
617 synapse elimination, and motor coordination. *Science*. 288:1832-1835.

618 Ito, M. 2002. Historical review of the significance of the cerebellum and the role of Purkinje
619 cells in motor learning. *Ann N Y Acad Sci*. 978:273-288.

620 Kakegawa, W., K. Tsuzuki, M. Iino, and S. Ozawa. 2003. Functional NMDA receptor
621 channels generated by NMDAR2B gene transfer in rat cerebellar Purkinje cells. *Eur J*
622 *Neurosci*. 17:887-891.

623 Kessels, H.W., S. Nabavi, and R. Malinow. 2013. Metabotropic NMDA receptor function is
624 required for beta-amyloid-induced synaptic depression. *Proc Natl Acad Sci U S A*.
625 110:4033-4038.

eNeuro Accepted Manuscript

626 Maher, B.J., and G.L. Westbrook. 2005. SK channel regulation of dendritic excitability and
627 dendrodendritic inhibition in the olfactory bulb. *J Neurophysiol*. 94:3743-3750.

628 Monyer, H., N. Burnashev, D.J. Laurie, B. Sakmann, and P.H. Seeburg. 1994. Developmental
629 and regional expression in the rat brain and functional properties of four NMDA
630 receptors. *Neuron*. 12:529-540.

631 Nabavi, S., H.W. Kessels, S. Alfonso, J. Aow, R. Fox, and R. Malinow. 2013. Metabotropic
632 NMDA receptor function is required for NMDA receptor-dependent long-term
633 depression. *Proc Natl Acad Sci U S A*. 110:4027-4032.

634 Nicoll, R.A., and R.C. Malenka. 1995. Contrasting properties of two forms of long-term
635 potentiation in the hippocampus. *Nature*. 377:115-118.

636 Peter, S., M.M. Ten Brinke, J. Stedehouder, C.M. Reinelt, B. Wu, H. Zhou, K. Zhou, H.J.
637 Boele, S.A. Kushner, M.G. Lee, M.J. Schmeisser, T.M. Boeckers, M. Schonewille,
638 F.E. Hoebeek, and C.I. De Zeeuw. 2016. Dysfunctional cerebellar Purkinje cells
639 contribute to autism-like behaviour in Shank2-deficient mice. *Nature communications*.
640 7:12627.

641 Piochon, C., T. Irinopoulou, D. Brusciano, Y. Bailly, J. Mariani, and C. Levenes. 2007.
642 NMDA receptor contribution to the climbing fiber response in the adult mouse
643 Purkinje cell. *J Neurosci*. 27:10797-10809.

644 Piochon, C., C. Levenes, G. Ohtsuki, and C. Hansel. 2010. Purkinje cell NMDA receptors
645 assume a key role in synaptic gain control in the mature cerebellum. *J Neurosci*.
646 30:15330-15335.

647 Piochon, C., H.K. Titley, D.H. Simmons, G. Grasselli, Y. Elgersma, and C. Hansel. 2016.
648 Calcium threshold shift enables frequency-independent control of plasticity by an
649 instructive signal. *Proc Natl Acad Sci U S A*. . 113:1091-6490.

650 Pugh, J.R., and I.M. Raman. 2006. Potentiation of mossy fiber EPSCs in the cerebellar nuclei
651 by NMDA receptor activation followed by postinhibitory rebound current. *Neuron*.
652 51:113-123.

653 Renzi, M., M. Farrant, and S.G. Cull-Candy. 2007. Climbing-fibre activation of NMDA
654 receptors in Purkinje cells of adult mice. *J Physiol*. 585:91-101.

655 Safo, P.K., and W.G. Regehr. 2005. Endocannabinoids control the induction of cerebellar
656 LTD. *Neuron*. 48:647-659.

657 Schonewille, M., A. Belmeguenai, S.K. Koekkoek, S.H. Houtman, H.J. Boele, B.J. van
658 Beugen, Z. Gao, A. Badura, G. Ohtsuki, W.E. Amerika, E. Hosy, F.E. Hoebeek, Y.
659 Elgersma, C. Hansel, and C.I. De Zeeuw. 2010. Purkinje cell-specific knockout of the
660 protein phosphatase PP2B impairs potentiation and cerebellar motor learning. *Neuron*.
661 67:618-628.

662 Schonewille, M., Z. Gao, H.J. Boele, M.F. Veloz, W.E. Amerika, A.A. Simek, M.T. De Jeu,
663 J.P. Steinberg, K. Takamiya, F.E. Hoebeek, D.J. Linden, R.L. Huganir, and C.I. De
664 Zeeuw. 2011. Reevaluating the role of LTD in cerebellar motor learning. *Neuron*.
665 70:43-50.

eNeuro Accepted Manuscript

666 Slemmer, J.E., C.I. De Zeeuw, and J.T. Weber. 2005. Don't get too excited: mechanisms of
667 glutamate-mediated Purkinje cell death. *Prog Brain Res*. 148:367-390.

668 Stahl, J.S., A.M. van Alphen, and C.I. De Zeeuw. 2000. A comparison of video and magnetic
669 search coil recordings of mouse eye movements. *Journal of neuroscience methods*.
670 99:101-110.

671 Tovar, K.R., and G.L. Westbrook. 2017. Modulating synaptic NMDA receptors.
672 *Neuropharmacology*. 112:29-33.

673 Voges, K., B. Wu, L. Post, M. Schonewille, and C.I. De Zeeuw. 2017. Mechanisms
674 underlying vestibulo-cerebellar motor learning in mice depend on movement
675 direction. *J Physiol*.

676 Wang, D.J., L.D. Su, Y.N. Wang, D. Yang, C.L. Sun, L. Zhou, X.X. Wang, and Y. Shen.
677 2014. Long-term potentiation at cerebellar parallel fiber-Purkinje cell synapses
678 requires presynaptic and postsynaptic signaling cascades. *Journal Neurosci.* 34:2355-
679 2364.

680 Wood, M.W., H.M. VanDongen, and A.M. VanDongen. 1996. The 5'-untranslated region of
681 the N-methyl-D-aspartate receptor NR2A subunit controls efficiency of translation.
682 *The Journal of biological chemistry*. 271:8115-8120.

683 Wulff, P., M. Schonewille, M. Renzi, L. Viltono, M. Sassoe-Pognetto, A. Badura, Z. Gao,
684 F.E. Hoebeek, S. van Dorp, W. Wisden, M. Farrant, and C.I. De Zeeuw. 2009.
685 Synaptic inhibition of Purkinje cells mediates consolidation of vestibulo-cerebellar
686 motor learning. *Nat Neurosci*. 12:1042-1049.
687
688
689

eNeuro Accepted Manuscript

Figure 1. Generation of NR2B transgenic mice. ***A,*** Schematic representation of the expression of endogenous NMDARs at CF-PC and PF-synapses over the wildtype mouse lifetime. All experiments performed in the following figures are performed at 6±1 weeks of age (see methods for details). *Middle*: scheme depicting the expression of NMDAR (dots) in a wildtype mouse at the synapses formed on the Purkinje cell (PC) dendritic tree by climbing fibers (cf). Synapses formed by parallel fibers (PF, the axons of granule cells, GC) do not have NMDARs. *Right*: same schematic representation of synapses onto Purkinje cells in the L7-NR2B+Tg transgenic mouse. Note that NMDARs are present also at the PF-PC synapse. *Inset*: Details of the vector used to generate the two independent lines used in the study. ***B,*** Western blot gels containing homogenates of adult cerebella, forebrains and hippocampi of two transgenic mice (Tg1+ and Tg2+) and their control littermates (Tg1- and Tg2-). The left blot was processed with an anti-NR2B antibody, which visualizes a band at 190kDa, the right one with an anti-NR1 antibody (120kDa). Actin was used as loading control; note that the ratio of NR-labeling to actin labeling should be taken into account for assessing the amounts of protein present. ***C,*** Confocal immunfluorescent images of of NR2B-immunoreactivityin dorsal hippocampus (Hip) and cerebellar cortex (Cb) in control (left), Tg1 (middle) and Tg2 (right) mice. Note in control mice, the low level of NR2B-labelling in the cerebellum as compared to hippocampal CA1 and dentate gyrus (DG). In addition note moderate increased labelling in cerebellar molecular layer (ml) of transgenic mice. ***D,*** Low- and high magnification images of Calbindin immunoreactivity in sagittal cerebellar sections illustrating the normal appearance of cerebellar gross morphology and Purkinje cells of adult transgenic (Tg1 and Tg2) mice. ***E,*** Top: high magnification of individual Golgi-stained Purkinje cells (black) of Control (left) as well as Tg1 (middle) and Tg2 (right) NR2B mice, counterstained with thionin (blue). Bottom: Sholl analysis of the dendritic arborization of Purkinje cells (left) and length of their primary dendrites (right) for control (black, n=30, N = 4), Tg1 (orange, n=30, N = 3) and Tg2 (red, n=30, N = 4) NR2B mice. Empty circles indicate individual data points, full circles indicate mean ± SEM.

Figure 2. Functional NMDARs are present at 6 weeks of age and do not compromise PCs' basic electrophysiological properties. ***A,*** *Left*: schematic

eNeuro Accepted Manuscript

representation of the recording configuration. *Middle:* example traces of CF currents recorded in the presence of the AMPA antagonist NBQX (green) and subsequently of blockers of both AMPA and NMDARs (D-AP5, black) in PCs of both transgenic lines and control littermates. Bold lines are average values; shading indicates individual cell variability. *Right*: quantification of NMDA current at the CF-PC synapse in control (Ctrl, black, n=5) and transgenic animals (Tg1, orange, n=7; Tg2, red, n=6). ***B,*** Similar to C, with additional example traces of baseline PF-evoked EPSCs before the addition of glutamatergic receptors blockers (blue), and normalized PF-PC NMDA current quantification (Ctrl, n=9; Tg1, n=9; Tg2, n=7). Note that NMDA-mediated currents are only significantly different from controls in Tg2. ***C,*** Average firing frequency elicited by somatic current injections from -65 mV in PCs of transgenic (Tg1, orange, n=5; Tg2, red, n=12) and control (Ctrl, black, n=15) mice. The inset illustrates the recording configuration. ***D,*** Average amplitude of the excitatory postsynaptic currents (EPSCs) at the PF-PC synapse to stimuli of increasing intensity for transgenic (Tg1, orange, n=5; Tg2, red, n=8) and control (Ctrl, black, n=18) mice. The inset illustrates the recording configuration**.** Empty circles represent individual data points, full circles are mean ± SEM; * indicates $p < 0.05$, ** indicates $p < 0.01$, and absolute *p*-values are indicated in the main text.

Figure 3. PF-PC LTP is selectively affected in transgenic mice. ***A,*** Long-term potentiation (LTP) was induced by PF stimulation at 1 Hz for 5 min in 6-week old transgenic (Tg2, red, n=8) and control (Ctrl, black, n=7) mice. The normalized paired-pulse ratio (50 ms inter-stimulus interval) of the recordings of the same cells is plotted below. ***B***, LTD was induced as described in ***A***, but with concomitant climbing fiber activation (Ctrl, n=8; Tg2, n=8). ***C,*** Similar to ***A***, but with the NMDAR blocker D-AP5 present in the extracellular solution (Ctrl, n=7; Tg2, n=8). ***D***, Induction of intrinsic plasticity by 5 min of PF stimulation at 1 Hz did not result in significant differences between transgenic and control mice (both N = 6). The normalized membrane potentials of the same cells are represented below. The scheme at the left of each panel depicts the respective recording configuration, while the middle example traces of Ctrl (black) and Tg2 (red) EPSCs (A-C) or action potentials (D) recorded before (t = 0 min) and after the tetanic stimuli (t = 20 min) show the plastic changes. Values

eNeuro Accepted Manuscript

are mean ± SEM; * indicates $p < 0.05$; ** indicate $p < 0.01$; absolute *p*-values are indicated in the main text.

4. Motor performance is normal, but motor learning is impaired in transgenic mice. ***A,*** Distance traveled and average speed in the open field for transgenic (Tg2, red, n=8) and control (Ctrl, black, n=7) mice. ***B-D,*** Baseline compensatory eye movements (examples traces for 0.4 Hz, middle left) quantified by gain (middle right) and phase (right) for Tg2 mice (red, n=9) and control (Ctrl, black, n=10) mice: (B) optokinetic reflex (OKR); (C) vestibulo-ocular reflex (VOR in the dark); and (D) visually-enhanced VOR (VVOR in the light), schematized on the right of each respective panel. ***E,*** Left: representation of gain-decrease training paradigm (day one: 5 × 10 min sinusoidal, *in phase* drum and table rotation at 0.6 Hz, both with an amplitude of 5°; day two: VOR gain measurement at 0.6 Hz). Middle: example traces of before (timepoint, t = 0, indicated by *a*) and after (t = 50 min, *b*) adaptation. *Right*: normalized gain for VOR recorded with 10 min intervals during 50 min training session for 6 weeks old Tg2 mice (red, n=8) and control (Ctrl, black, n=11) mice on day one and a single measurement at day two. ***F,*** Similar to ***E***; following the gain-decrease protocol, for 4 consecutive days the 6 weeks old transgenic and control mice were subjected to the phase reversal protocol (5 × 10 min sinusoidal *in-phase* drum and table rotation at 0.6 Hz, but with drum amplitudes of 7.5° on day 2 and 10° on days 3-5, while the table amplitude was 5°). VOR responses (middle: example traces, *a* same as ***E***, *c*: t = 50 min on day 4) are depicted as gain of eye movement multiplied by the cosine of its phase, gain*cos(phase). Negative values here indicate a phase larger than 90° and the (theoretical) goal of the training is a value of -1. Empty circles represent individual data points, full circles are mean ± SEM; *p*-values are indicated in the main text; asterisks indicate significant difference.

eNeuro Accepted Manuscript

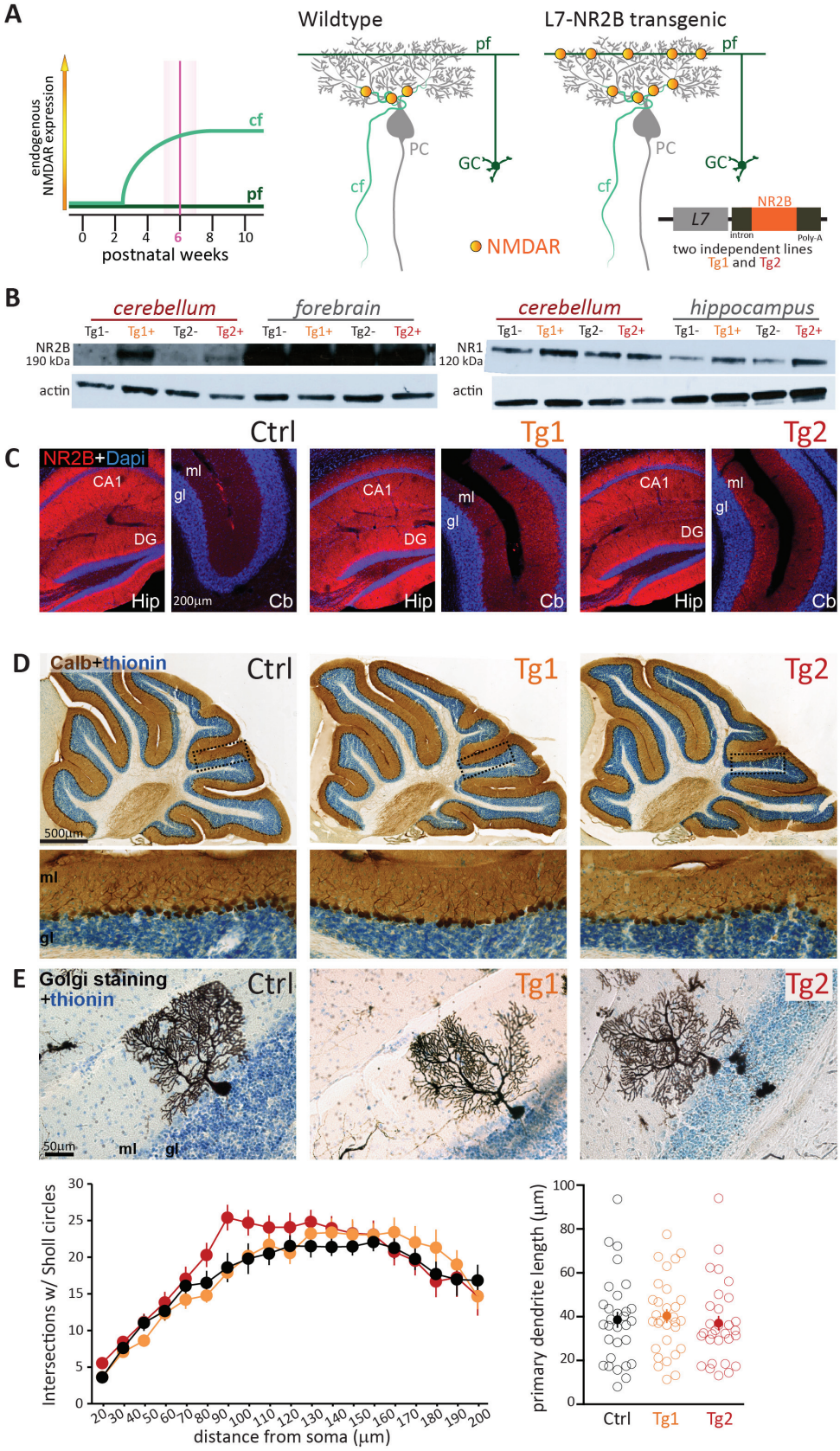

Figure 1

eNeuro Accepted Manuscript

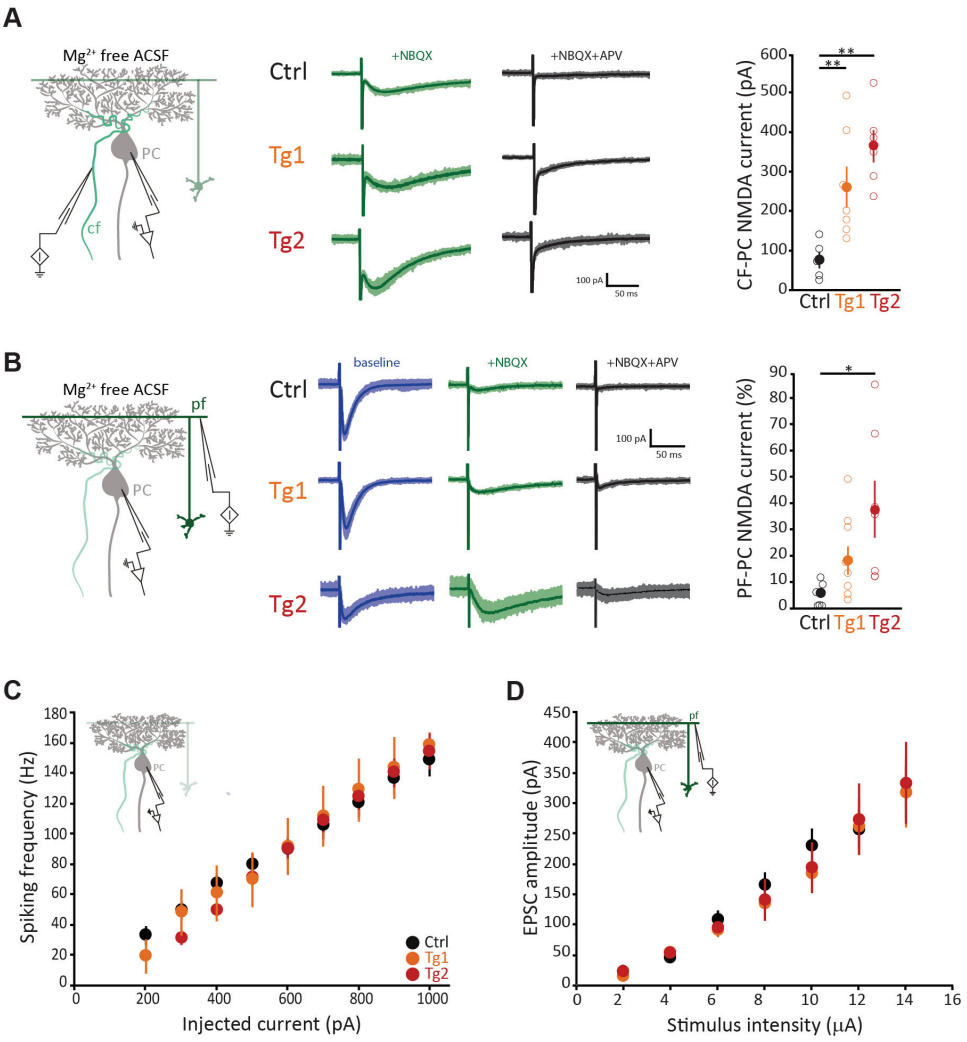

Figure 2

eNeuro Accepted Manuscript

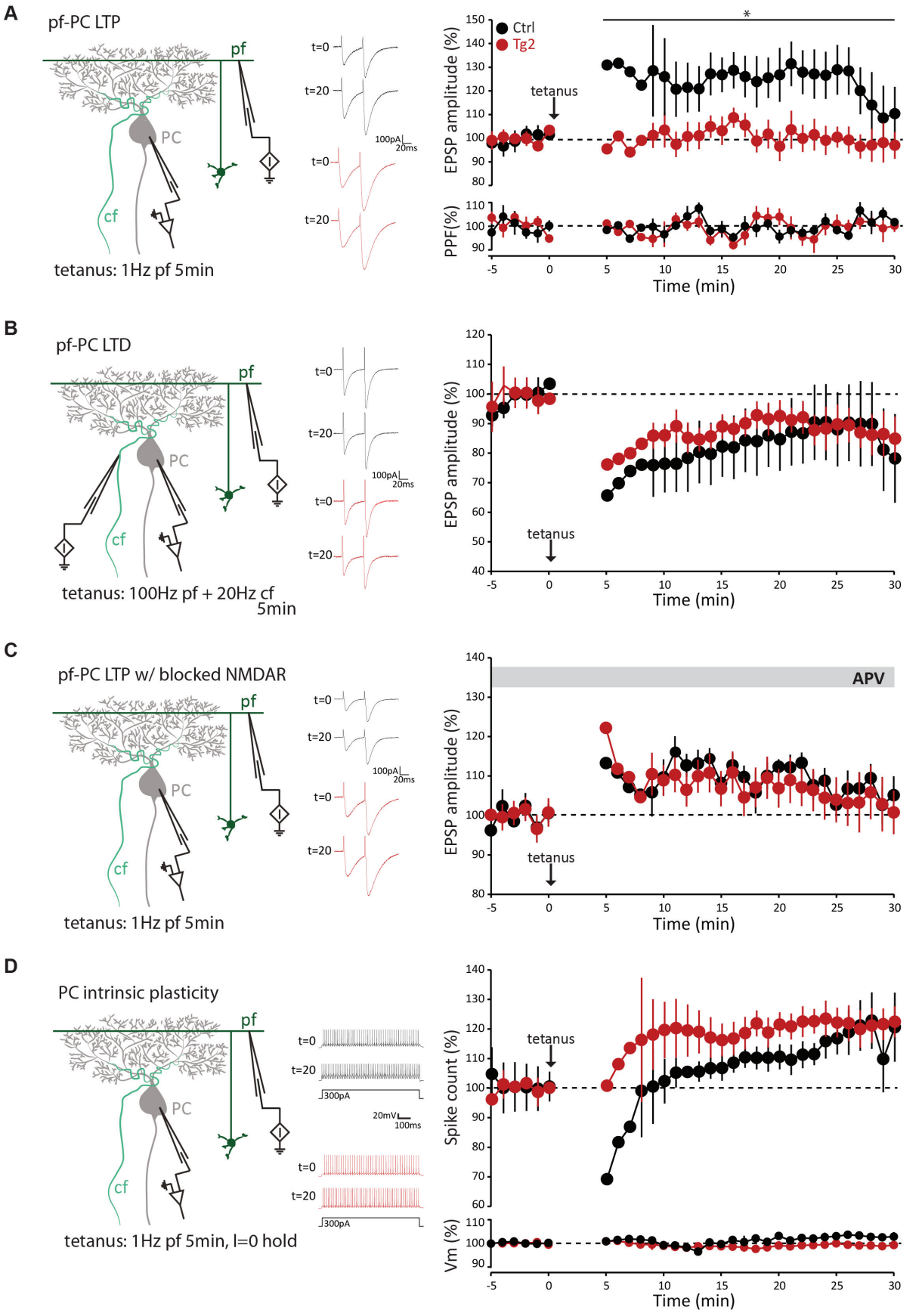

Figure 3

eNeuro Accepted Manuscript

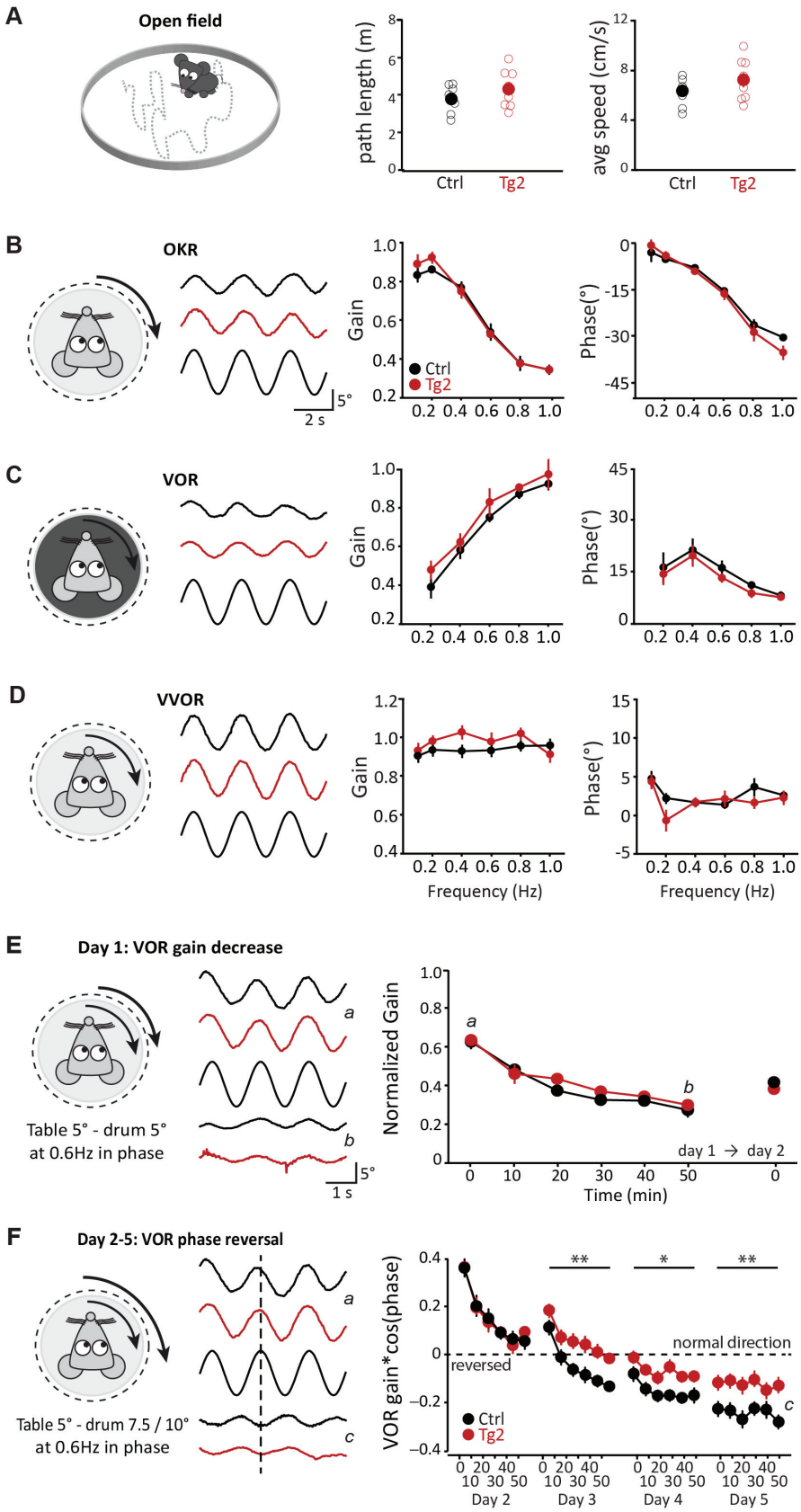

Figure 4